Iranian Journal of Medical Physics

ijmp.mums.ac.ir

# Quality Assurance of LINAC by Analyzing the Profile of 6-MV and 10-MV Photon Beams Using Star Track Device

Basma Sabr Lazim[1], Basim Khalaf Rejah[2*], Haydar H. Alabedi[3]

1. Ministry of Education, Baghdad, Iraq
2. Department of physics College of Science for Women, University of Baghdad, Baghdad, Iraq
3. Ministry of Health and Environment, Baghdad Radiotherapy and Nuclear Medicine, Center Baghdad, Iraq

ARTICLE INFO

*Article type:*
Original Article

*Article history:*
Received: Apr 29, 2019
Accepted: Jul 13, 2019

*Keywords:*
Linear Accelerator
Star Track
Radiation Therapy
Iraq

ABSTRACT

***Introduction:*** According to the American Society of Radiation Oncology, all patients receive radiation therapy during their illness, where radiation is delivered by the medical linear accelerator (Linac). The aim of this study was to evaluate the quality assurance (QA) of the Linac in analyzing the used dose profile in the treatment of cancer tumors.

***Material and Methods:*** This experimental study was performed using Linac (synergy device type) at Baghdad Radiotherapy and Nuclear Medicine laboratories, Baghdad, Iraq. The Star Track device was used for the routine quality assurance of the Linac, using photon beam for the reference $D_{max}$ and source to surface distance of 100 cm. The Star Track consists of 453 vented parallel plate ionization chambers.

***Results:*** The flatness and symmetry of beams for the reference field size did not exceed from ±2%, as they were within the allowed range. Moreover, the penumbra region showed a change in value that did not exceed from ±0.2 cm. using the Star Track method; maximum differences in beam symmetry and beam flatness were measured at 0.76%±2% and 1.17%±2%, respectively. Moreover, the maximum difference in the penumbra region was estimated at 0.12±0.2 cm.

***Conclusion:*** The results indicated, the Star Track could successfully calculate the characteristics of dose profile during a time period of 2,500 ms, showing the superiority of this instrument over other verification devices.

► *Please cite this article as:*
Lazim B.S, Rejah B.Kh, Alabedi HH. Quality Assurance of LINAC by Analyzing the Profile of 6-MV and 10-MV Photon Beams Using Star Track Device. Iran J Med Phys 2020; 17: 260-265. 10.22038/ijmp.2019.39987.1543.

## Introduction

The linear accelerator (Linac) machine produces photon energy higher than 6 MV [1]. Linear accelerators modify high-vitality X-beams or electrons to adjust to tumor shape and kill malignant cells, while saving the surrounding normal tissues. The Linac is a device that uses electromagnetic waves to accelerate charged particles, such as elevating the electron kinetic energy from 4 MeV to 25 MeV [2-3].

It is prescribed that the quality assurance of beam energy for radio therapeutic machines is performed at customary interims, either weekly or monthly. Therefore, the purpose of using quality assurance machines is to measure the actual dose, and then compare it with the reference value. Quality assurance procedures are designed to minimize the difference between the prescribed and delivered dose [4-8].

Real segments of quality confirmation projects manage the safe precision of dose conveyance to the right target volume. Quality assurance tests should be carried out intermittently to guarantee the deviations in dosimetry, as well as mechanical and wellbeing parameters, are inside specific resistance.

Mistakes can emerge from numerous components, including mechanical breakdown after some time and faulty electronics.

The quality procedure program is based on the recommendations of the American Association of Physicists [9-12]. In radiotherapy, dose variations are distributed in tumors, although these variations must remain within the permissible limits. In IEC protocol, the flatness, symmetry, and penumbra are defined at $D_{max}$ [13, 14].

### *Beam profiles of the radiation beam*

The axis data are given where beam profiles are measured perpendicular to the beam central axis at a given depth. The depth measurements inside the machine are typically at $D_{max}$ [15, 16]. If we need information about the dissemination of the dose outside the central axis, we should use the dose profile. Dose profile uniformity is usually measured by scan along the center of the beam. Three parameters that quantify field uniformity are determined as beam symmetry, beam flatting, and penumbra region, which are described as:

**Corresponding Author:* Tel: +96 47731757520; E-mail: basimkr_phys@csw.uobaghdad.edu.iq

Flatness is defined as the ratio of the maximum absorbed dose in the radiation field to the minimum absorbed dose in the flattened area at the standard depth of measurement and is calculated using *Equation (1)*:

$$F.B = \frac{d_{max}-d_{min}}{d_{max}+d_{min}} \times 100\% \quad (1)$$

Beam symmetry of radiation is referred to as the maximum ratio of the absorbed dose measurement at points located at equidistant from the radiation beam axis, up to 80% of the field size [17] and is calculated using *Equation (2)*:

$$S.B= \frac{a_{right}-a_{left}}{a_{right}+a_{left}} \times 100 \quad (2)$$

Penumbra regions are defined as the areas near the edge of the field where the dose is in a growing and decreasing state. This area can be defined more accurately as a lateral distance between 80% and 20% of the maximum dose points at one side of the beam profile. The measurement of this area is calculated at the same time for both symmetry and flattening photon beams [18, 19].

## Materials and Methods

***Star Track***

This experimental study was conducted at Baghdad Radiotherapy and Nuclear Medicine Center, Baghdad, Iraq. All data measurements were made by the Star Track device for the routine validation of the quality assurance of photon or electron beam radiation outside the Synergy Linac, which was used for managing cancerous tissue. The Star Track machine according to the Omni Pro-Advance Users Guide consists of 453 vented parallel plate ionization chambers. The distance between ionization detectors is 5 mm. The ionization counter diameter is approximately 3 mm. The machine power supply module can be connected to the main power with the voltage ranging from 100 to 240 V.

In the Star Track device, the chambers were arranged in horizontal, vertical, and diagonal lines as shown in Figure 1.

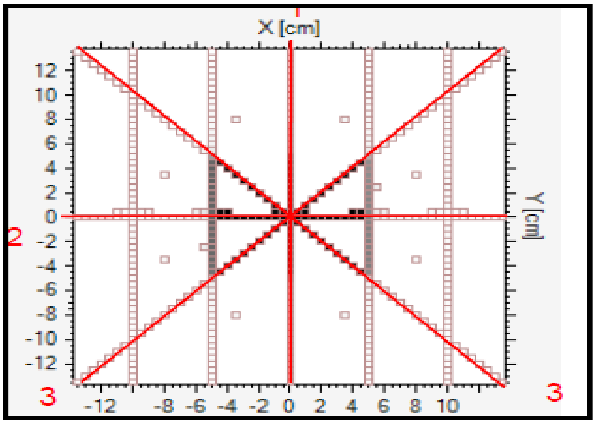


Figure 1. Detectors in the Star Track device.

Table 1. Characteristics of the detectors in the Star Track device

| | |
|---|---|
| Active Area | 27×27 cm, measuring field sizes up to 25×25 cm |
| Chamber size | Cylindrical, 3 (Ø)×5 (h) mm, Sensitive volume 0.035 cm³ |
| Sensor layout | Chamber arrays organized along the main axes and diagonals, additional 4 arrays parallel to the lateral main axis, 10 additional chambers for energy constancy check |

Additionally, the characteristic of the detectors in the Star Track device is shown in Table 1.The released charge in the active volume of the chambers was separated by an electrical field between the bottom and top electrodes. The collected current that was proportional to the dose rate was measured and digitized by an individual electrometer for each chamber. For the purpose of achieving the quality assurance procedure, dose profile was measured using the energies of 6 MV and 10 MV for photon beams towards the x-axis, by the sophisticated Star Track machine, in addition, the measured dose was compared to the reference values.

The purpose behind using the Star Track device was to evaluate the performance of this instrument in evaluating the quality assurance of the Linac in analyzing the dose profile of photon or electron beams in comparison to that of other verification devices, such as phantom, which reduces time and effort.

***Measurement of dose profile by the Star Track method***

All dose profile measurements were performed at a source to surface distance (SSD) of 100 cm and depth of $D_{max}$. In these measurements, the Star Track was placed on the treatment couch, precisely under the Linac head; then, the Star Track was moved to a distance of 100 cm (distance from the Linac source to the device surface). Afterward, the Star Track was connected to the electrical source and the computer outside the examination room (Figure 2). Inline profiles (x-axis) were scanned at the $D_{max}$ for a field size of 10×10 cm using photon beams in this study. Flatness and symmetry of the beams were well-defined in 80% of the full width at half of the maximum area of the profile dose.

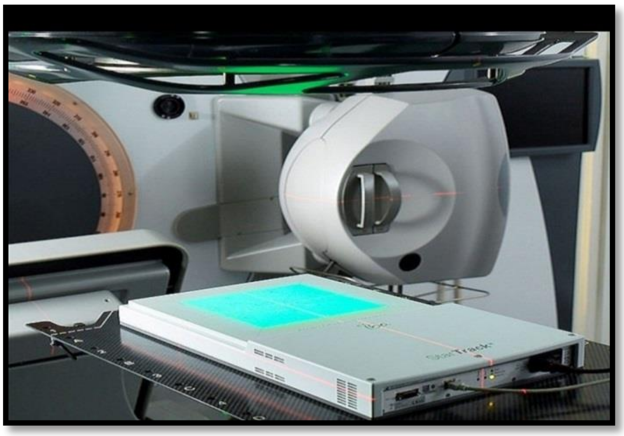

Figure 2. Star Track system, IBA dosimetry

Table 2. Device operation conditions

| Conditions | |
|---|---|
| Temperature | +15 - +35 Ċ |
| Pressure | 500- 1,100 h pa |
| Relative humidity | 30-70% without condensation |
| Power supplied | 100-240 V |

***Linear accelerator***

The Synergy Linac device was installed at Baghdad Radiotherapy and Nuclear Medicine Center as shown in Figure. 3. This system was capable of generating X-rays in the range of megavoltage and delivering dual energies of 6 and 10 MV.

Figure3. Synergy linear accelerator device at Baghdad Radiotherapy and Nuclear Medicine Center, Baghdad, Iraq

## Results

***Photon beam***

***Analysis of dose profiles***

A field with a size of 10×10 cm and photon beam energies of 6 and 10 MV at $D_{max}$ was selected for this study. Figures 4 and 5 illustrate the dose profile using 6 and 10 MV at $D_{max}$. The data extracted from the curves show the dose characteristics using the Star Track method (Table 3). The results in Table 3 show the measured dose profile in the obtained and referenced reading with minimum differences. This value did not exceed from ±2% and ±0.2 cm for beam flatness/beam symmetry and penumbra region, respectively, during the first week.

Figures 6 and 7 depict the dose profile using 6 and 10 MV at $D_{max}$. The data extracted from the curves show the characteristics of the dose using the Star Track method (Table 4). The result in Table 4 depicts the measured dose profile in the obtained and referenced reading with minimum differences. As the results indicated, this value did not exceed from ±2% and ±0.2 cm for beam flatness/beam symmetry and penumbra region, respectively, during the second week.

The penumbra value on the right-hand side using 6 MV was similar to the reference value. In addition, the value of penumbra on the left-hand side sing 10 MV was identical to the reference value, as shown in Table 4. Figures 8 and 9 illustrate the dose profile using 6 and 10 MV at $D_{max}$. The data extracted from the curves show the dose characteristics using the Star Track method (Table 5). Table 5 presents the measured dose profiles in the obtained and referenced reading with minimum differences. This value did not exceed from ±2% and ±0.2 cm for beam flatness/beam symmetry and penumbra region, respectively, during the third week. In addition, the value on the right-hand side penumbra using 6 MV showed similarity to the reference value (Table 5).Figures 10 and 11 display the dose profile using 6 and 10 MV at $D_{max.}$ The data extracted from curves by the Star Track method show dose characteristics (Table 6). Table 6 present the measured dose profiles in the obtained and referenced reading with minimum differences. The value did not exceed from ±2% and ±0.2 cm for beam flatness/beam symmetry and penumbra region, respectively, during the fourth week.

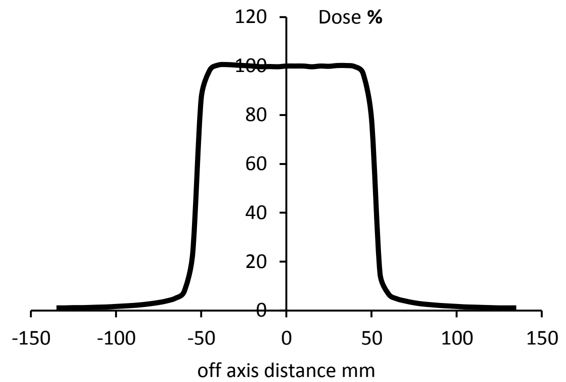


Figure 4. Dose profile graph in the direction of x-axis using 6 MV for a field size of 10×10 $cm^2$ during the first week of using the Star Track method

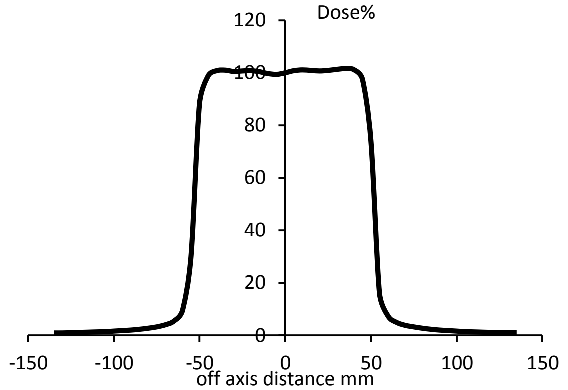


Figure 5. Dose profile graph in the direction of x-axis using 6 MV for a field size of 10×10 $cm^2$ during the first week of using the Star Track method

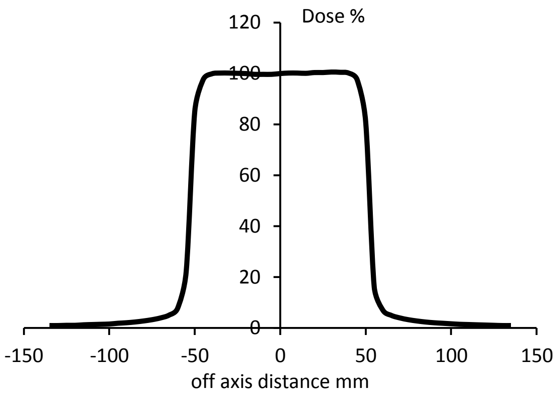


Figure 6. Dose profile graph in the direction of x-axis using 6 MV for a field size of 10×10 cm$^2$ during the second week of using the Star Track method

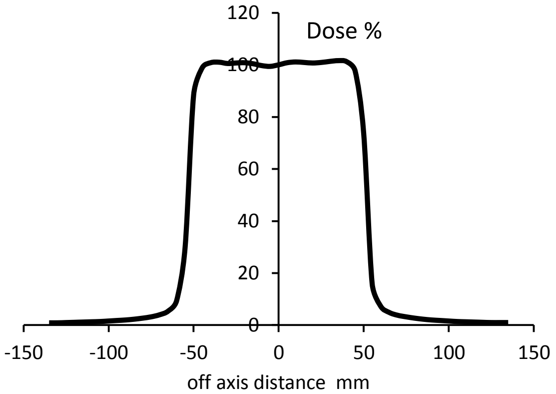


Figure 7. Dose profile graph in the direction of x-axis using 6 MV for a field size of 10×10 cm$^2$ during the second week using the Star Track method

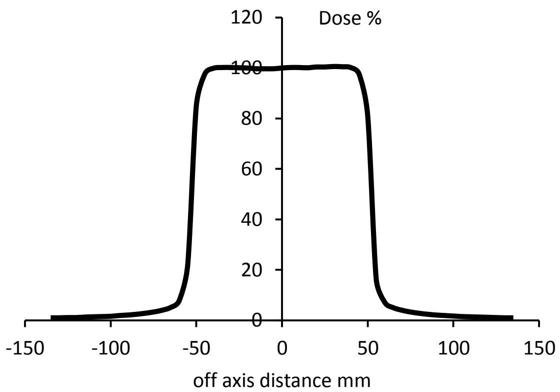


Figure 8.Dose profile graph in the direction of x-axis using 6 MV for a field size of 10 ×10 cm$^2$ during the third week of using the Star Track method

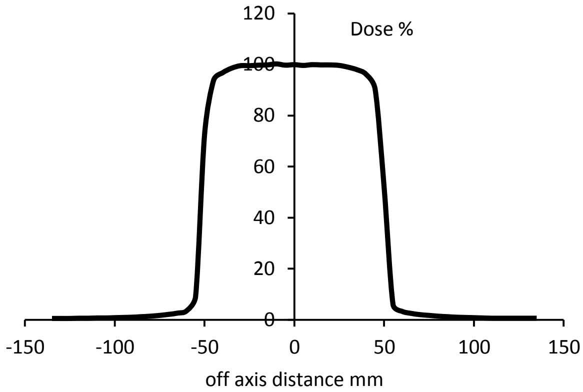


Figure 9. Dose profile graph in the direction of x-axis using 10 MV for a field size of 10×10 cm$^2$ during the third week of using the Star Track method

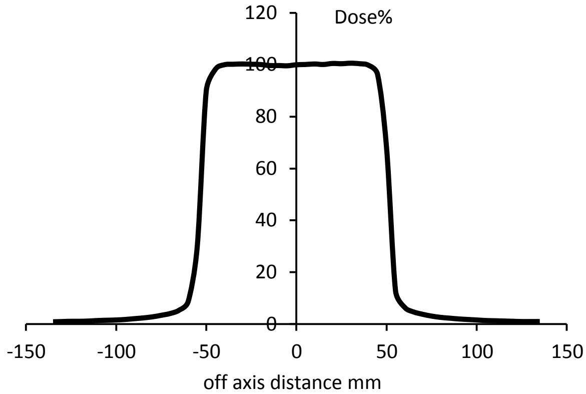


Figure 10. Dose profile graph in the direction of x-axis using 6 MV for a field size 10×10 cm$^2$ during the fourth week of using the Star Track method

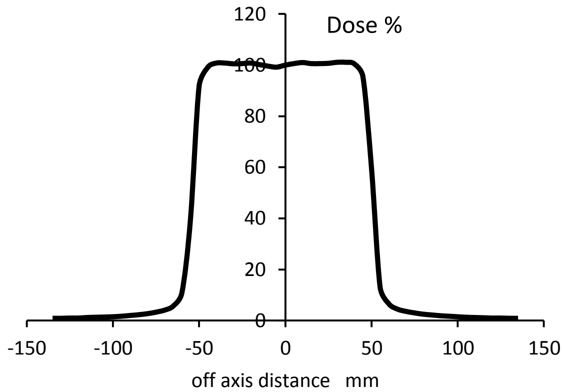


Figure11. Dose profile graph in the direction of x-axis using 10 MV for a field size of 10×10 cm$^2$ during the fourth week of using the Star Track method

Table 3 . Dose profile parameters using 6 and 10 MV for a field size of 10×10 cm$^2$ by the Star Track device in the first week

| Dosage characteristics toward x-axis, 6 MV | | | | Dosage characteristics toward x-axis, 10 MV | | | |
|---|---|---|---|---|---|---|---|
| Test | Result | Reference | Dif. | Test | Result | Reference | Dif. |
| P.L | 0.56cm | 0.53cm | 0.03 | P.L | 0.68cm | 0.67cm | 0.01 |
| P.R | 0.50cm | 0.46cm | 0.04 | P.R | 0.63cm | 0.59cm | 0.04 |
| B.F | 101.69% | 101.36% | 0.33 | B.F | 101.96% | 102.1% | -0.14 |
| B.S | 100.74% | 100.38% | 0.36 | B.S | 101.30% | 101.35% | -0.05 |

P.L: left-hand side penumbra, P.R: right-hand side penumbra, BF: beam flatness, BS: beam symmetry

Table 4. Dose profile parameters using 6 and 10 MV for a field size of 10×10 $cm^2$ by the Star Track device in the second week

| Dosage characteristics toward x-axis, 6 MV | | | | Dosage characteristics toward x-axis, 10 MV | | | |
|---|---|---|---|---|---|---|---|
| Test | Result | Reference | Dif. | Test | Result | Reference | Dif. |
| P.L | 0.48cm | 0.53cm | -0.05 | P.L | 0.66cm | 0.67cm | -0.01 |
| P.R | 0.46cm | 0.46cm | 0 | P.R | 0.61cm | 0.59cm | 0.02 |
| B.F | 102.53% | 101.36% | 1.17 | B.F | 101.74% | 102.1% | -0.36 |
| B.S | 101.14% | 100.38% | 0.76 | B.S | 101.14% | 101.35% | -0.21 |

P.L: left-hand side penumbra, P.R: right-hand side penumbra, B.F: beam flatness, B.S: beam symmetry

Table 5. Dose profile parameters using 6 and 10 MV for a field size of 10×10 $cm^2$ by the Star Track device in the third week

| Dosage characteristics toward x-axis, 6 MV | | | | Dosage characteristics toward x-axis, 10 MV | | | |
|---|---|---|---|---|---|---|---|
| Test | Result | Reference | Dif. | Test | Result | Reference | Dif. |
| P.L | 0.65cm | 0.53cm | 0.12 | P.L | 0.73cm | 0.67cm | 0.06 |
| P.R | 0.65cm | 0.46cm | 0.19 | P.R | 0.71cm | 0.59cm | 0.12 |
| B.F | 101.61% | 101.36% | 0.25 | B.F | 102.00% | 102.1% | -0.1 |
| B.S | 100.56% | 100.38% | 0.18 | B.S | 101.47% | 101.35% | 0.12 |

P.L: left-hand side penumbra, P.R: right-hand side penumbra, B.F: beam flatness, B.S: beam symmetry

Table 6. Dose profile parameters using 6 and 10 MV for a field size of 10×10 $cm^2$ by the Star Track device in the fourth week

| Dosage characteristics toward x-axis, 6 MV | | | | Dosage characteristics toward x-axis, 10 MV | | | |
|---|---|---|---|---|---|---|---|
| Test | Result | Reference | Dif. | Test | Result | Reference | Dif. |
| P.L | 0.54cm | 0.53cm | 0.01 | P.L | 0.67cm | 0.67cm | 0 |
| P.R | 0.46cm | 0.46cm | 0 | P.R | 0.60cm | 0.59cm | 0.01 |
| B.F | 101.75% | 101.36% | 0.39 | B.F | 102.26% | 102.1% | 0.16 |
| B.S | 100.5% | 100.38% | 0.12 | B.S | 101.42% | 101.35% | 0.07 |

P.L: left-hand side penumbra, P.R: right-hand side penumbra, B.F: beam flatness, B.S: beam symmetry

## Discussion

### *Photon beams dose profile*

The dose profile parameters measured by the Star Track method were in agreement with the dose profile parameters referenced for 6 and 10 MV photon beams, respectively. The dose profiles parameters showed a very good match with the reference value by the Star Track method for reference depth. In addition, the values of beams edge (penumbra region) were matched very well with the referenced value using the Star Track method. The dose profile parameters determined by the Star Track method for 6 and 10 MV at a field size of 10×10 cm and SSD of 100 cm are shown in the provided figures.

The results showed a maximum difference in the symmetry and flatness of beams at 0.76%±2% and 1.17% ±2%, respectively. A little distinction in dose was found between the left and right penumbra regions, whereas the maximum difference in the penumbra region was measured at 0.12±0.2 cm. This confirms the stability of the Star Track machine in the validation of the quality assurance of the Linac by analyzing the dose profile of photon beams (6 and 10 MV) over 4 weeks.

## Conclusion

The quality assurance program of the radiotherapy division remained the fundamental perspective for the nature of the treatment just as for the security of the conveyed dose using the Star Track methods. The penumbra region with symmetry and flatness beams established essential attributes for the photon beam results obtained from the analysis of the dose profile by the Star Track methods, which were compatible with the reference values. These results did not exceed the permissible limits with the difference between references. Additionally, the resulting value did not exceed from ±2% for beam flatness and symmetry and 0.2 cm for the penumbra region. The Star Track system was able to verify the quality of the Linac through the analysis of the dose profiles.

## Acknowledgment

The researchers would like to extend their gratitude to Baghdad Radiotherapy and Nuclear Medicine Center, Baghdad, Iraq, for evaluating the Linac quality using the Star Track device.

## References

1. Shrotriya D, Yadav S, Lal Srivastava N. Surface Dose Measurements on an Indigenously Made Inhomogeneous Female Pelvic Phantom. Using Metal-Oxide-Semiconductor-Field-Effect-Transistor Based Dosimetric System. Iran J Med Phys. 2018; 15(4): 304-7.
2. Krabch M, Chetaine A, Saidi K, Errad FT, Nourreddine A, Benkhouya Y, et al. Measurements of Photon Beam Flattening Filter Using an Anisotropic Analytical Algorithm and Electron Beam Employing Electron Monte Carlo.Iran J Med Phys. 2019;16(6):200-9.
3. Pathak P, Mishra PK, Singh M, Mishra PK. Cancer Science & Therapy Analytical Study of Flatness and Symmetry of Electron Beam with 2D array detectors. journal of cancer science and therapy. 2015;7(10):294‑301.
4. Hanley J, Bayouth J. Task Group 142 report: quality assurance of medical accelerators. Med Phys. 2009; 36 (9):4197‑212.
5. Farrukh S, Ilyas N, Naveed M, Haseeb A, Bilal M. Penumbral dose characteristics of physical and virtual wedge profiles. international journal of medical physics. 2017; 6: 216‑24.
6. Hegazy EA . Evaluation of using radiographic films in measurements of penumbra width for radiotherapy applications evaluation of using radiographic films in measurements of penumbra width for radiotherapy applications. Journal of advancesin physics. 2018;14(1):5204-12.
7. Das J, Cheng W, Watts R, Ahnes J, Gibbons X, Lowenstein Li, et al. Report of the TG-106 of the Therapy Physics Committee of the AAPM: Accelerator beam data commissioning equipment and procedures. J Medical Physics. 2008; 35: 4186‑215.
8. Patatoukas GD, Kalavrezos P, Seimenis I, Dilvoi M, Efstathopoulos E, Platoni K. Determination of beam profile characteristics in radiation therapy using different dosimetric set ups. JBUON. 2018; 23(5):1448‑59.
9. Enoch M, Mcdonald K. Dose distribution in 3D water phantom and profiler 2 scanning system. IJSBAR. 2017; 34 (3) : 149-57.
10. Speight RJ, Esmail A, Weston SJ. Quality assurance of electron and photon beam energy using the BQ-Check phantom.journal of appled clincal medical physics. 2011;12 (2): 293-44 .
11. Pereira GC, Traughber M, Muzic RF. The Role of imaging in radiation therapy planning: past, present, and future. Biomed Res Int. 2014 ;2: 1‑9.
12. Billan S, Charas T , Billan S, Charas T. External beam radiation in differentiated thyroid arcinoma. Rambam Maimonides. Med J. 2016; 7(1): 1-6.
13. Yorke E, Gelblum D, Ford E. Patient safety in external beam radiation therapy. Am J Roentgenol. 2011 ; 196 (4) :768‑72.
14. Khan FM. the Physics of radiation therapy. 4th ed. williams & wilkins. 2010;33-45.
15. Diamantopoulos S, Thalassinou S. In vivo dosimetry in the field junction area for 3D-conformal radiation therapy in breast and head & neck cancer cases: A quality assurance study. JBUON. 2016; 21:1104-12.
16. Yarahmadi M, Nedaie HA, Allahverdi M, Asnaashari KH, Sauer OA .Small photon field dosimetry using EBT2 Gafchromic film and Monte Carlo simulation. Int J Radiat Res. 2013; 11(4):215-24.
17. Khan FM. the physicie of radiation therapy.5thed .wolters klvwer. 2014;413-20.
18. Ravichandran R, Binukumar JP, Davis CA, Krishnamurthy K, Sivakumar SS. Evaluation methods for detecting changes in beam output and energy in radiation beams from high-energy linear Accelerators. Med Phys. 2007; 32 (3):5-40.
19. Tajiki S, Nedaie HA, Esfehani M, Geraily Gh, Hassani M, Rastjoo A, et al. Penumbra Measurements and Comparison of In-House and Standard Circular Cones by the Gafchoromic Film Pinpoint Ion Chamber, and MCNPX Monte Carlo Simulation. Iran J Med Phys. 2019; 16(3):232-40.